Controlled Angiogenesis in Peptide Nanofiber Composite Hydrogels

Navindee C. Wickremasinghe[†], **Vivek A. Kumar**[†], **Siyu Shi**[†], and **Jeffrey D. Hartgerink**[*,†,‡]

[†]Department of Chemistry, Rice University, Bioscience Research Collaborative, 6500 Main Street, Houston, Texas 77030, United States

[‡]Department of Bioengineering, Rice University, Bioscience Research Collaborative, 6500 Main Street, Houston, Texas 77030, United States

Abstract

Multidomain peptide (MDP) nanofibers create scaffolds that can present bioactive cues to promote biological responses. Orthogonal self-assembly of MDPs and growth-factor-loaded liposomes generate supramolecular composite hydrogels. These composites can act as delivery vehicles with time-controlled release. Here we examine the controlled release of placental growth factor-1 (PlGF-1) for its ability to induce angiogenic responses. PlGF-1 was loaded either in MDP matrices or within liposomes bound inside MDP matrices. Scaffolds showed expected rapid infiltration of macrophages. When released through liposomes incorporated in MDP gels (MDP(Lipo)), PlGF-1 modulates HUVEC VEGF receptor activation in vitro and robust vessel formation in vivo. These loaded MDP(Lipo) hydrogels induce a high level of growth-factor-mediated neovascular maturity. MDP(Lipo) hydrogels offer a biocompatible and injectable platform to tailor drug delivery and treat ischemic tissue diseases.

Abstract
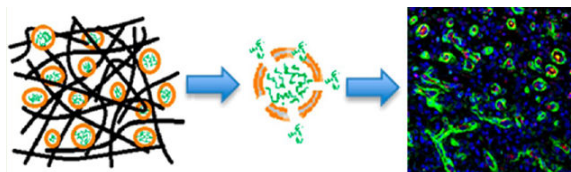
Keywords

self-assembly; multidomain peptide; liposomal encapsulation; PlGF-1; cellular infiltration; angiogenesis

INTRODUCTION

Therapeutic angiogenesis is critical for the salvage of ischemic tissue.[1,2] The lack of blood flow (ischemia) to tissue causes development of low oxygen environments (hypoxia). Ensuing from this is retention of proinflammatory cytokines, waste products, high CO_2 microenvironments, and consequent tissue necrosis.[3] Similarly, to enhance tissue regeneration beyond the diffusion limit, new blood vessel growth, neoangiogenesis, is required.

Current strategies to induce blood vessel growth include growth factor delivery, cell therapy, matrix interaction, and metabolic control.[3] Growth factors (GFs) affecting angiogenesis such as VEGF,[4,5] FGF,[2] PlGF,[6,7] and PDGF[8] have been delivered to ischemic tissue in a variety of methods to stimulate vascularization. Emerging therapies employ multiple GFs to control cellular infiltration and create niches for blood vessel formation.[9,10] Transplantation of allo-/ autologous bone marrow stromal cells, mesenchymal stem cells, and endothelial progenitor cells has been attempted with modest success; the need for multiple surgeries and the proliferative potential of these cells are of concern.[3,>11–>13] Cell therapy has been combined with bioactive materials designed to closely mimic the natural extracellular matrix (ECM).[3,14,15] Administration of nitrite/ nitric oxide to ischemic tissue increases expression of VEGF; concerns over systemic and local side effects and stability have limited this technique.[3,16,17] There are three critical features of angiogenesis that need to be addressed: (1) retention of nascent vessels, (2) development of mature vessels, and (3) resorption of excessive or unnecessary vasculature.[1] These factors promote an environment that supports growing vessels that are stabilized by pericytes, buttressed by smooth muscle cells, and resorb without creating chronic inflammatory sites.[15]

Multidomain peptides (MDPs) offer a method to enhance therapeutic angiogenesis and can be used to address the above three features.[15,18–22] MDPs have multiple domains (hydrophilic, hydrophobic, charged) that aid in self-assembly to nanofibers.[18,23] These amphiphiles assemble by eliminating water in their hydrophobic regions, forming hydrogen bonding networks wherein fiber length is controlled by terminal charge repulsion.[24,25] With the addition of multivalent ions (such as PO_4^{3-}), charge repulsion is overcome by shielding, allowing growth of long-range ECM mimetic nanofibers.[1–3] These hydrophilic nanofibers entangle, forming hydrogels. Self-assembly by noncovalent interactions allows shear thinning and recovery and consequent injectability.[15,22,26] MDPs have also been shown to have antimicrobial behavior[27] and can also be modified for a variety of biological activities.[15,28] Specific to angiogenesis, we have developed a MDP covalently bound to a mimic of VEGF-165. This peptide, termed SLanc, results in rapid cellular infiltration and a high degree of angiogenesis.[15] In contrast to covalent immobilization above, in this work, we used a complementary approach to obtain in vivo angiogenesis: orthogonal assembly of MDP and liposomes, with a proangiogenic growth factor. Achieving similar levels of angiogenesis with this strategy demonstrates its facile nature for delivery of a variety of GFs with distinct effects. Additionally, temporal control of growth factor delivery may allow tuning of angiogenic responses.

Two recent studies have demonstrated the tailoring of immune responses in a temporal fashion as a function of growth factor/cytokine delivery.[28,29] The MDP in this study, termed SLac, has a sequence of KSLSLSLRGSLSLSLKGRGDS.[18,20,21] It contains a cell adhesion fibronectin-derived (RGD) moiety promoting infiltration. Further, SLac has a central matrix metal-loproteinase (MMP) cleavage sequence (LRG) allowing biodegradation.[4,5,18]

We have previously shown that MDPs are rapidly infiltrated by cells as observed in subcutaneous injections in rats. After just 3 days, millimeter-sized scaffolds showed unprecedented infiltration into the center of scaffolds.[15,26] We have demonstrated the release of cytokines to modulate inflammatory environments by activating prohealing M1 macrophages, specifically IL-4.[28] The success of these SLac hydrogels in tailoring inflammatory processes guided the use of MDP scaffolds for angiogenesis. Tailoring of time-controlled release of GFs and cytokines utilizing MDP scaffolds may allow more precise control of in vivo responses. As proof of principle, and of most relevance here, is our recently reported work involving the two-step self-assembly of a composite hydrogel for temporal release of bioactive factors.[22] This composite system consisted of MDPs and growth factors encapsulated by liposomes and are termed here as MDP–Liposome Composites (MLCs).

Liposomes offer a number of advantages for drug delivery and have been used for many decades as vehicles for delivery.[5,30–32] The lipid bilayer in liposomes mimics the cellular plasma membrane. Degradation of liposomes can be caused by fusion of liposomal membranes to cell membranes, engulfment of liposomes by cells, and/or collapse of liposomes due to instability.[22,30] Time delay of cargo release caused by encapsulation in liposomes may allow dictation of a variety of stimuli in composite systems. The liposomes synthesized in the above study were 100 ± 50 nm in size and displayed a PlGF-1 loading efficiency of approximately 60%. Orthogonal self-assembly of these loaded liposomes and MDPs into a higher order structure (Figure 1) have been shown to drive controlled release, while providing an ECM mimetic environment.[22] We published a drug delivery method capitalizing on liposomes as carriers of GF molecules, which could be expanded to a broad spectrum of proteins or small molecules. Release studies with MLCs involving bioactive factors MCP-1, EGF, and PlGF-1 demonstrated bimodal release in vitro: burst release from the MDP matrix alone and delayed release from MLCs (liposomes incorporated inside MDPs).[22] Thus, we were able to achieve temporal control in release, dependent on discharge by liposomes.[22] We have demonstrated maintenance of bioactivity after release and stability of growth factors in MDP matrices.[28] We believe MLCs are unique in that they provide a more generalized delivery strategy for bimodal controlled release, largely independent of the entrapped material.[30] Additionally, MLCs have proven to be more effective in delivery than liposomes alone due to their ability to localize the released load (targeted injection) and stabilize the surrounding environment via cellular infiltration.

In this study, we investigated three different hydrogel systems for their potential to serve as scaffolds for cellular infiltration and angiogenesis (Table 1). Hydrogels were loaded with placental growth factor-1 (PlGF-1). PlGF-1 is a key angiogenic and vasculogenic factor, reported to stimulate angiogenesis by direct and indirect mechanisms via its ability to bind and activate VEGFR-1.[6,7,9,33–35] Although it has not been studied as extensively as VEGF,

Luttun et al. and Autiero et al. have indicated the proangiogenic potential of PlGF-1 in ischemic heart and limb models with comparable efficacy to VEGF.[6,7,33,34] The use of PlGF-1 here was prompted by studies that have demonstrated its potential in forming large mature, durable vessels (arteriogenesis) that persist for prolonged periods, while indicating no complications such as edema, hyperpermeability, and hemangioma genesis observed with VEGF.[33,36–38]

Depending on the method in which PlGF-1 is incorporated, we hypothesized marked differences in the in vivo response. Specifically, we hypothesized that controlled release can tailor cellular recruitment and neovascularization. PlGF-1 was incorporated into the hydrogels in two ways: in the MDP matrix, MDP(PlGF-1), and inside liposomes of the MLCs, MDP(Lipo(PlGF-1)). This allowed evaluation of delayed release for formation and stabilization of blood vessels, in and around the implant site. We hypothesized that initial cellular recruitment to the implant will form a niche for the subsequent infiltration and stabilization of blood vessels. Furthermore, we hypothesized that delayed release of PlGF-1 (after completion of cellular infiltration) would be superior to burst release from MDP alone.

The work presented herein shows that temporal control in PlGF-1 release leads to the development of robust, mature vasculature. Notably, no signs of fibrous encapsulation, hematomas, or hemorrhaging were observed. The materials and methods described in this study may provide a powerful tool in the arsenal of therapies used in regenerative medicine, a tool that bridges nascent leaky vessels, immature and small capillaries, and ultimately demonstrates facile control of neoangiogenesis. More importantly, this represents an exciting approach wherein highly biocompatible materials tailor tissue responses[39] through orthogonal self-assembly and biphasic release.

EXPERIMENTAL SECTION

Synthesis and Characterization of MDP

MDP with the sequence K(SL)$_3$RG(SL)$_3$KGRGDS (SLac) was synthesized on a low loading Rink amide MBHA resin on a 0.15 mM scale using a Focus XC automated solid-phase peptide synthesizer (Aapptec, Louisville, KY) by using an optimized protocol reported previously.[18] Peptide was cleaved from the resin using a mixture of TFA, triisopropylsilane, water, ethanedithiol, and anisole in a 36:1:1:1:1 ratio. Resulting peptide had neutralized termini due to the acetylated N-terminus and amidated C-terminus. Cleaved peptide was rotoevaporated, precipitated in cold ether, and dried overnight. Crude peptide was dissolved in Milli-Q water to form a 1 wt % solution and pH adjusted to 7.4 prior to dialysis (MWCO 500–1000 Da) for 3 days with buffer changes twice daily. Postdialysis, the peptide solution was frozen and lyophilized. Synthesis of the correct peptide was confirmed by matrix-assisted laser desorption/ionization time-of-flight (Bruker Daltonics, Billerica, MA) mass spectroscopy (MALDI-TOF). Secondary structure analyzed by circular dichroism was published previously.[22]

Synthesis of Liposomes and Encapsulation of PlGF-1

Phospholipids and cholesterol were purchased from Avanti Polar Lipids, Inc. Dipalmitoylphosphatidylcholine (DPPC), dipalmitoylphos-phatidylglycerol (DPPG), and

cholesterol were mixed in chloroform in the molar ratio of 5:1:4, and the solvent was evaporated by passing nitrogen. The dried lipids were left under high vacuum overnight to allow complete evaporation of chloroform. Encapsulation of PlGF-1 was carried out in situ during the hydration phase of liposome preparation. Dry lipid films were hydrated with 1 μg/mL solution of human recombinant PlGF-1 (PeproTech, Rocky Hill, NJ) in carrier-free HBSS (Life Technologies, Carlsbad, CA). The mixture was sonicated briefly and incubated for 1 h with intermittent agitation. Then it was subjected to five freeze–thaw cycles and extruded through a 100 nm polycarbonate membrane using a Mini-Extruder (Avanti Polar Lipids Inc., Alabaster, AL). Afterward, the unencapsulated PlGF-1 was removed by passing the liposome suspension through a Sephadex G-75 column. The efficiency of encapsulation of PlGF-1 has been calculated as 62% in previously published release studies.[22] Liposomes were sized by dynamic light scattering experiments performed on a Malvern Zen 3600 Zetasizer (Malvern Instruments Ltd., Malvern, UK).[22]

In Vitro PlGF-1 Release from MDP–Liposome Composite Gel

Lyophilized SLac peptide was dissolved at 20 mg/mL in Milli-Q water with 298 mM sucrose, and the pH was adjusted to 7.4. The MDP–liposome composite gel was made by mixing 100 μL of purified PlGF-1-entrapped liposomes with 100 μL of 20 mg/mL SLac. According to the encapsulation efficiency, approximately 60 ng of PlGF-1 was loaded in each gel. Fifteen such MDP–liposome gels were made (5 gels per time point) in a 24-well plate. Each gel was topped with 1.5 mL of supernatant media (Medium 200 with 1% FBS from Life Technologies) and incubated at 37 °C and 5% CO_2 for 10 days. At time points day 2, day 5, and day 10, 1 mL of the release media was removed and frozen at −80 °C until human umbilical vein endothelial cells (HUVECs) were ready for treatment.

Assessment of Angiogenic Receptor Activation in HUVECs by PlGF-1 Release

HUVECs (Life Technologies) were seeded in 6-well plates at 2×10^5 cells per well and cultured in full media (Medium 200 with 10% LVES from Life Technologies) overnight. Cells were then starved for 24 h in low serum media (Medium 200 with 0.5% LVES). PlGF-1 release aliquots obtained at each time point in release study were added to cells and kept for another 24 h. Two controls were tested: (1) negative control with only low serum media and (2) positive control with 1 mL of a 100 ng/mL solution of PlGF-1. PCR was used to characterize HUVEC phenotypic expression, $n = 5$ for three independent repeats. RNA extraction was performed according to manufacturer's protocol (RNeasy, Qiagen, Gaithersburg, MD). RNA concentrations were determined using Nanodrop (Thermo Scientific, Waltham, MA), and reverse transcription to cDNA was carried out using iScript (Qiagen), followed by RT-PCR using a Biorad CFX96 Real-Time PCR machine (Biorad, Berkeley, CA) and SsoAdvanced SYBR-green KIT (Qiagen). PCR primers were purchased from Life Technologies. Primers used: vascular endothelial growth factor receptor 1, VEGFR-1 forward: 5-TCCCTTATGATGCCAGCAAGT-3, VEGFR-1 reverse: 5-CCAAAAGCCCCTCTTCCAA-3; vascular endothelial growth factor receptor 2, VEGFR-2 forward: 5-CACCACTCAAACGCTGACATGTA-3, VEGFR-2 reverse: 5-GCTCGTTGGCGCACTCTT-3; housekeeping ribosomal 60s subunit L37a forward primer: ATTGAAATCAGCCAGCACGC, L37a reverse primer: AGGAACCACAGTGCCAGATCC. CT values generated by the software were compared to

L37a expression. Expression of the gene of interest was normalized to control expression (media control) noted in each experiment.

In Vivo Subcutaneous Implants in Rats

All experiments were approved by the Rice University Institutional Animal Care and Use committee. Female Wistar rats (225–250 g, Charles River Laboratories, Wilmington, MA) were anesthetized using isofluorane (2% for induction and 1% for maintenance) and dorsal aspects shaved under sterile conditions. Three different hydrogels were made ($n = 4$ for each gel) and loaded in syringes with 22 gauge needles. The gels were prepared as follows:

1. MDP alone (SLac): 20 mg/mL SLac mixed with HBSS in 1:1 ratio

2. MDP(PlGF-1): 20 mg/mL SLac mixed with 1 μg/mL of recombinant rat PlGF-1 (PeproTech) made in HBSS, in 1:1 ratio.

3. MDP(Lipo(PlGF-1)): 20 mg/mL SLac mixed with rat PlGF-1-encapsulated liposomes (containing approximately 60 ng PlGF-1) made in HBSS, in 1:1 ratio.

Two hundred microliter subcutaneous injections were made in four separate 1.5 in. spaced randomized sites on the dorsal aspect, on either side between the lower thoracic and upper lumbar vertebrae. At tested time points day 2, day 5, and day 10, rats were euthanized using an overdose of isoflurane, CO_2 asphyxiation, and bilateral thoracic puncture. The dorsal skin around the entire implant was removed, washed with PBS, and fixed in neutral buffered formalin for 24 h prior to processing.

Evaluation of Cellular Infiltrate, Neomatrix Development, and Angiogenesis

Tissue was processed to paraffin blocks, sectioned at 7 μm, deparaffinized, and stained for cellular infiltrate using H&E. Masson's Trichrome staining was carried out according to manufacturer's instructions (Sigma-Aldrich, St. Louis, MO) to visualize collagen deposition. Cellular infiltrate was determined using immunostaining for macrophages: rabbit anti-rat CD68+ (Abcam, Cambridge, UK), and nucleic DAPI counterstain. Angiogenic evaluation was performed by immunostaining for endothelial cells: rabbit anti-rat vWF+ (ABCam), biotin anti-rat Lectin+ (Santa Cruz Biotechnology, Dallas, TX); smooth muscle cells: rabbit anti-rat α-SMA+ (Dako, Carpenteria, CCA), mouse anti-rat α-SMA+ (Abcam); pericytes: mouse anti-rat Nestin+ (Millipore, Darmstadt, Germany) and nucleic DAPI counterstain. Secondary antibodies used were donkey anti-rabbit AF 647, goat anti-mouse FITC, streptavidin AF 647 (Life Technologies), donkey anti-rabbit AF 568. Cellular infiltrate was quantified by counting DAPI-stained nuclei and cells stained as macrophages using ImajeJ software. Angiogenesis was quantified by determining vessel density (vessels per unit area, $n = 4$ separate sections, $n = 4$ samples).

Statistical Analysis

Data are represented as mean ± SD. One-way ANOVA was conducted for multiple comparisons of parametric data, with Tukey post-hoc analysis for all pairwise comparisons of the mean responses to the different treatment groups. Values of $p < 0.05$ were considered to be statistically significant.

RESULTS AND DISCUSSION

Temporal Control of PlGF-1 Release Leads to Controlled Activation of Angiogenic Receptors

In vitro angiogenic marker expression of HUVECs was quantified by RT-PCR in response to PlGF-1 release. Release media aliquots at days 2, 5, and 10 resulted in upregulation of canonical angiogenic marker VEGFR-1 and VEGFR-2 expression. Receptor upregulation was normalized to ribosomal housekeeping gene L37a.[15,40] Day 2 expression levels were not immediately upregulated to a significant extent (Figure 2). Peak expression is seen at day 5 with a decrease by day 10. This suggests that signaling by PlGF-1 is delayed past day 2, due to liposomal release occurring around day 3, affirming GF release previously reported.[22] VEGFR-1 and VEGFR-2 upregulation is critical for angiogenesis.[7,9,34] These results suggest that in vivo angiogenesis can be tailored temporally by employing MLCs to delay angiogenic stimuli. Loading of PlGF-1 in the matrix resulted in more immediate receptor upregulation compared to delayed liposomal release in MDP-(Lipo(PlGF-1)).

Rapid Infiltration of Cells Precedes Vessel Formation

In vivo implantation of MLCs was performed under the dorsal subcutaneous aspect of Wistar rats (Figure S1). Composite gels 2 and 3 presented PlGF-1 in the matrix and PlGF-1 within liposomes, respectively (Figure 1). Harvested tissue at days 2, 5, and 10 was fixed and embedded. H&E and immunostaining was used to determine cellular infiltrate. Identification of the implant was facilitated by cellular density and hydrogel morphology (Figure S2). Representative images at day 2 showed high levels of cellular infiltration into each of the implants, irrespective of GF presence (Figure 3). This is in congruence with previous studies of MDP/SLac.[15,28] Cellular density within implants was maintained at days 5 and 10 (Figures S3–S5). Cytotaxis is either through MMP-mediated scaffold degradation, phagocytosis, or physical motility through soft injectable gels.[18,20,28] Cellular infiltration in unloaded gels demonstrates MDP potential for molecular reorganization and provision of a cytocompatible niche.

Further, from H&E sections and Masson's Trichrome staining (Figure 4), it can be reasoned that high cellular infiltration seems to play a crucial role in preventing a thick fibrous encapsulation. It also indicates that the implant remains accessible to migrating cells and is not walled off from the rest of the tissue, restricting direct contact with cells, as is usually the case when a thick fibrous capsule forms and actively prevents cells from migrating into the implant.[41–43] The seamless interface of native tissue and composite hydrogels demonstrates excellent tissue integration (Figures 3 and S2–S4). Additionally, no gross signs of inflammation (redness, swelling, altered gait/function) were observed, indicating minimal rejection by the host. This suggests that the host animal responds to the present artificial matrix as if it were native extracellular matrix. There are very few materials that exhibit no fibrous encapsulation.[15,44,45] As per our design strategy, early infiltrating cells may provide a suitable niche for the stabilization of nascent vasculature induced by delayed PlGF-1 release.[15]

Characterizing the cellular infiltrate helped identify specific cell types that promote robust vascular formation. Immunofluorescent staining showed CD68+ macrophages in all scaffolds (Figures 3 S4). While CD68+ macrophages were present in all hydrogels at day 2, a higher number of macrophages were observed in the composite gels loaded with PlGF-1, compared to SLac alone. By day 5, macrophage counts for all scaffolds were similar, tapering by day 10 (Figure 3 and Figures S4 and S5). Resolution of the initial macrophage response potentially provides a niche for angiogenesis in MLCs, mimicking native tissue healing mechanisms of acute wounds.

Collagen staining using Masson's Trichrome helped visualize the degradation of implant over time (Figures 4 and S6). At day 5, the edges of the implant show disintegration, and collagen deposition is found along the same edges as well as in the center of the implant, in some cases. Day 10 images indicate more collagen deposition with the size of the implant shrinking. It appears that a significant portion of the implant has degraded, and it is replaced by new matrix, which can be distinguished from the native fascia by the blue color of the collagen staining.

Development of Robust Vasculature

Two separate panels of markers were used to determine angiogenesis: (1) panel A: endothelial marker (vWF+; red), smooth muscle marker (α-SMA+; green) counterstained with DAPI; (2) panel B: endothelial marker (Lectin+; purple), pericyte marker (Nestin+; green), smooth muscle marker (α-SMA+; red) counterstained with DAPI. Angiogenesis showed dependence on PlGF-1 release (Figure 5). PlGF-1 releases rapidly from the matrix,[22] resulting in nascent vessel-like structures defined only by a lining of endothelial cells. Early release of PlGF-1 from the hydrogel matrix signals immature and low vessel development in the short term (Figures 6 and S8). Incorporating PlGF-1 in liposomes delays its release up to 3 days, at which point liposomes lyse, releasing their load.[22] Thus, the onset of angiogenesis is triggered immediately after that in MLCs. By day 5, many vessels in various stages of development are seen in MLCs. Day 5 implants of MLCs demonstrate robust angiogenesis in contrast to MDP(PlGF-1) gels releasing PlGF-1 directly from the matrix (Figure 6).

These MDP(Lipo(PlGF-1)) implants show the highest vessel density and the greatest number of vessels lined with pericytes and smooth muscle cells (Figure 5). Nascent vessels start to regress, leaving fewer but more mature vessels at day 10. As a result, the total vessel density decreases at day 10, although the presence of mature vessels is still significantly high (Figure 5–7). The fascia is not a region that is naturally vascularized. As the hydrogel degrades, we believe that excess vessels are also removed by resorption, so that the newly deposited matrix is made to closely mimic the native fascia, which normally has a low vessel density. Encapsulation of PlGF-1 in liposomes with delayed release after macrophage recruitment shows the most robust vessel development within 5 days. In summary, blood vessel development begins after 2 days and is most numerous at the 5 day time point, with retention of mostly robust mature vessels at the day 10 time point (Figures 7 and 8).

Comparison to Previous Angiogenesis Attempts

MLCs loaded with growth factors were shown to elicit a controlled immune response and tailor angiogenic responses. Clinical outcomes for therapeutic revascularization have been met with modest success with current techniques. VEGF delivery via plasmid vector or whole growth factor has resulted in leaky vasculature, potential neoplasticity, and inadequate clinical improvement.[46–48] Stem cell therapy has been used to attempt neovascularization. Ongoing clinical trials have shown modest results, with some groups suggesting that cell death causes a proinflammatory response that stimulates tissue growth.[3,15,48]

Use of growth factor release to modulate angiogenesis has been shown previously.[2,4–8] The degree and maturity of the vessels that developed have been modest, compared to the neovasculature seen in this study. For example, VEGF delivery from PEG-based hydrogels has demonstrated high levels of VEGF release in the first two days with a gradual decrease over the next 2 weeks.[46] The composites in this study have been shown to release PlGF-1 after 3 days,[22] allowing cellular infiltration to occur prior to PlGF-1 release triggering angiogenesis. Alternative strategies have used engineered variants of VEGF conjugated to fibrin matrices for sustained release, resulting in nonleaky vasculature.[49,50] This delivery strategy is encumbered by growth factor modification and optimization for matrix binding. Liposomal carriers offer delayed release of a variety of GFs in a tailorable fashion without the need for chemical modification.[30–32,51–53]

Self-assembling peptide hydrogels have been used previously for GF delivery.[54,55] RADA16 has been utilized for delivery of EGF,[56] PDGF-BB,[57] SDF-1,[58] and IGF-1.[59] Although these approaches have been met with appreciable success, our system differs in its modular nature. The use of liposomal carriers allows for long-term and delayed delivery of therapeutics. Further, initial in vivo studies have shown the rapid degradation of the RADA16 within 3–7 days, compared to the persistence of MLCs for over 2 weeks.[15,28]

This delivery strategy can be improved with encapsulation of a variety of drugs, growth factors, and cytokines in microspheres,[60] micelles,[61,62] and nanoparticles[63,64] and possibly covalent conjugation[65] for release in the long term as well as multiple GF delivery.[10,66] Additionally, we and others have demonstrated the ability to use heparin binding domains to attenuate release from MDP.[20,62,67]

MLCs can serve as matrices for tissue regeneration to treat a milieu of pathologies potentially including peripheral vascular disease, diabetic ulcers, and tissue infarcts.[48] Future in vivo experiments in disease models will better help guide the utility of MLCs in clinically relevant settings. We have demonstrated the ability to tailor and modulate inflammation to one of an M2 healing/pro-angiogenic phenotype from MDP.[28] We have also shown the ability to abrogate adverse tissue reactions by passive loading of MDP. Given the synergistic nature of MLCs and their ability to temporally control tissue responses, as demonstrated in this study, we envision a series of models in ischemic tissue disease that can benefit from these approaches.[2,6,48]

CONCLUSION

In this study, we have presented a technique to fabricate MLCs that modulate angiogenesis. MLCs with PlGF-1 loaded in the liposome component showed temporal control of in vitro angiogenic receptor activation. When MLCs with PlGF-1 loaded in the liposomes were injected subcutaneously in rats, MLCs showed spatial and temporal control of angiogenesis. These hydrogels showed high levels of cellular infiltration, creating a suitable environment for large stable microvasculature promoted by PlGF-1 release. The biological response observed by time-controlled release from these supramolecular constructs is directly dependent on structural aspects of MLCs. These constructs were rationally designed, with the intent of developing a system that can mimic the level of complexity seen in sophisticated natural systems. MLCs were engineered with multiple components capable of displaying orthogonal self-assembly and the subsequent time-controlled release.[22]

Supplementary Material

Refer to Web version on PubMed Central for supplementary material.

ACKNOWLEDGMENTS

REFERENCES

1. Freedman SB. Therapeutic Angiogenesis for Coronary Artery Disease. Ann. Intern. Med. 2002; 136(1):54. [PubMed: 11777364]

2. Losordo DW, Dimmeler S. Therapeutic angiogenesis and vasculogenesis for ischemic disease. Part I: angiogenic cytokines. Circulation. 2004; 109(21):2487–2491. [PubMed: 15173038]

3. Phelps EA, Garcia AJ. Update on therapeutic vascularization strategies. Regener. Med. 2009; 4(1): 65–80.

4. Sun Q, Chen RR, Shen Y, Mooney DJ, Rajagopalan S, Grossman PM. Sustained vascular endothelial growth factor delivery enhances angiogenesis and perfusion in ischemic hind limb. Pharm. Res. 2005; 22(7):1110–1116. [PubMed: 16028011]

5. Scott RC, Rosano JM, Ivanov Z, Wang B, Chong PL-G, Issekutz AC, Crabbe DL, Kiani MF. Targeting VEGF-encapsulated immunoliposomes to MI heart improves vascularity and cardiac function. FASEB J. 2009; 23(10):3361–3367. [PubMed: 19535683]

6. Luttun A, Tjwa M, Moons L, Wu Y, Angelillo-Scherrer A, Liao F, Nagy JA, Hooper A, Priller J, De Klerck B, et al. Revascularization of ischemic tissues by PlGF treatment, and inhibition of tumor angiogenesis, arthritis and atherosclerosis by anti-Flt1. Nat. Med. 2002; 8(8):831–840. [PubMed: 12091877]

7. Tjwa M, Luttun A, Autiero M, Carmeliet P. VEGF and PlGF: two pleiotropic growth factors with distinct roles in development and homeostasis. Cell Tissue Res. 2003; 314(1):5–14. [PubMed: 13680354]

8. Barrientos S, Stojadinovic O, Golinko MS, Brem H, Tomic-Canic M. Growth factors and cytokines in wound healing. Wound Repair Regen. 2008; 16(5):585–601. [PubMed: 19128254]

9. Carmeliet P, Moons L, Luttun A, Vincenti V, Compernolle V, De Mol M, Wu Y, Bono F, Devy L, Beck H, et al. Synergism between vascular endothelial growth factor and placental growth factor contributes to angiogenesis and plasma extravasation in pathological conditions. Nat. Med. 2001; 7(5):575–583. [PubMed: 11329059]

10. Richardson TP, Peters MC, Ennett AB, Mooney DJ. Polymeric system for dual growth factor delivery. Nat. Biotechnol. 2001; 19(11):1029–1034. [PubMed: 11689847]

11. Zhou L, Chen Z, Vanderslice P, So S-P, Ruan K-H, Willerson JT, Dixon RAF. Endothelial-like progenitor cells engineered to produce prostacyclin rescue monocrotaline-induced pulmonary arterial hypertension and provide right ventricle benefits. Circulation. 2013; 128(9):982–994. [PubMed: 23841984]

12. Madonna R, Ferdinandy P, De Caterina R, Willerson JT, Marian AJ. Recent developments in cardiovascular stem cells. Circ. Res. 2014; 115(12):e71–e78. [PubMed: 25477490]

13. Willerson JT, Taylor D, Perin EC. Till truth makes all things plain: human hearts and stem cells. Circ. Res. 2014; 115(11):908–910. [PubMed: 25378531]

14. Kocher AA, Schuster MD, Szabolcs MJ, Takuma S, Burkhoff D, Wang J, Homma S, Edwards NM, Itescu S. Neovascularization of ischemic myocardium by human bone-marrow-derived angioblasts prevents cardiomyocyte apoptosis, reduces remodeling and improves cardiac function. Nat. Med. 2001; 7(4):430–436. [PubMed: 11283669]

15. Kumar VA, Taylor NL, Shi S, Wang BK, Jalan AA, Kang MK, Wickremasinghe NC, Hartgerink JD. Highly angiogenic Peptide nanofibers. ACS Nano. 2015; 9(1):860–868. [PubMed: 25584521]

16. Kumar D, Branch BG, Pattillo CB, Hood J, Thoma S, Simpson S, Illum S, Arora N, Chidlow JH, Langston W, et al. Chronic sodium nitrite therapy augments ischemia-induced angio-genesis and arteriogenesis. Proc. Natl. Acad. Sci. U. S. A. 2008; 105(21):7540–7545. [PubMed: 18508974]

17. Lundberg JO, Weitzberg E, Gladwin MT. The nitrate-nitrite-nitric oxide pathway in physiology and therapeutics. Nat. Rev. Drug Discovery. 2008; 7(2):156–167. [PubMed: 18167491]

18. Galler KM, Aulisa L, Regan KR, D'Souza RN, Hartgerink JD. Self-assembling multidomain peptide hydrogels: designed susceptibility to enzymatic cleavage allows enhanced cell migration and spreading. J. Am. Chem. Soc. 2010; 132(9):3217–3223. [PubMed: 20158218]

19. Bakota EL, Aulisa L, Galler KM, Hartgerink JD. Enzymatic cross-linking of a nanofibrous peptide hydrogel. Biomacromolecules. 2011; 12(1):82–87. [PubMed: 21133404]

20. Galler KM, Hartgerink JD, Cavender AC, Schmalz G, D'Souza RN. A customized self-assembling peptide hydrogel for dental pulp tissue engineering. Tissue Eng., Part A. 2012; 18(1–2):176–184. [PubMed: 21827280]

21. Kang MK, Colombo JS, D'Souza RN, Hartgerink JD. Sequence effects of self-assembling multidomain peptide hydrogels on encapsulated SHED cells. Biomacromolecules. 2014; 15(6):2004–2011. [PubMed: 24813237]

22. Wickremasinghe NC, Kumar VA, Hartgerink JD. Two-step self-assembly of liposome-multidomain peptide nanofiber hydrogel for time-controlled release. Biomacromolecules. 2014; 15(10):3587–3595. [PubMed: 25308335]

23. Aulisa L, Dong H, Hartgerink JD. Self-assembly of multidomain peptides: sequence variation allows control over cross-linking and viscoelasticity. Biomacromolecules. 2009; 10(9):2694–2698. [PubMed: 19705838]

24. Dong H, Paramonov SE, Aulisa L, Bakota EL, Hartgerink JD. Self-assembly of multidomain peptides: balancing molecular frustration controls conformation and nanostructure. J. Am. Chem. Soc. 2007; 129(41):12468–12472. [PubMed: 17894489]

25. Bakota EL, Sensoy O, Ozgur B, Sayar M, Hartgerink JD. Self-assembling multidomain peptide fibers with aromatic cores. Biomacromolecules. 2013; 14(5):1370–1378. [PubMed: 23480446]

26. Bakota EL, Wang Y, Danesh FR, Hartgerink JD. Injectable multidomain peptide nanofiber hydrogel as a delivery agent for stem cell secretome. Biomacromolecules. 2011; 12(5):1651–1657. [PubMed: 21417437]

27. Xu D, Jiang L, Singh A, Dustin D, Yang M, Liu L, Lund R, Sellati TJ, Dong H. Designed supramolecular filamentous peptides: balance of nanostructure, cytotoxicity and antimicrobial activity. Chem. Commun. (Cambridge, U. K.). 2015; 51(7):1289–1292.

28. Kumar VA, Taylor NL, Shi S, Wickremasinghe NC, D'Souza RN, Hartgerink JD. Self-assembling multidomain peptides tailor biological responses through biphasic release. Biomaterials. 2015; 52:71–78. [PubMed: 25818414]

29. Kumar VA, Shi S, Wang BK, Li I-C, Jalan AA, Sarkar B, Wickremasinghe NC, Hartgerink JD. Drug-triggered and cross-linked self-assembling nanofibrous hydrogels. J. Am. Chem. Soc. 2015; 137(14):4823–4830. [PubMed: 25831137]

30. Samad A, Sultana Y, Aqil M. Liposomal drug delivery systems: an update review. Curr. Drug Delivery. 2007; 4(4):297–305.

31. Vemuri S, Rhodes C. Preparation and characterization of liposomes as therapeutic delivery systems: a review. Pharm. Acta Helv. 1995; 70(2):95–111. [PubMed: 7651973]

32. Li F, Sun J-Y, Wang J-Y, Du S-L, Lu W-Y, Liu M, Xie C, Shi J-Y. Effect of hepatocyte growth factor encapsulated in targeted liposomes on liver cirrhosis. J. Controlled Release. 2008; 131(1): 77–82.

33. Luttun A, Tjwa M, Carmeliet P. Placental Growth Factor (PlGF) and Its Receptor Flt-1 (VEGFR-1). Ann. N. Y. Acad. Sci. 2002; 979(1):80–93. [PubMed: 12543719]

34. Autiero M, Waltenberger J, Communi D, Kranz A, Moons L, Lambrechts D, Kroll J, Plaisance S, De Mol M, Bono F, et al. Role of PlGF in the intra- and intermolecular cross talk between the VEGF receptors Flt1 and Flk1. Nat. Med. 2003; 9(7):936–943. [PubMed: 12796773]

35. De Falco S. The discovery of placenta growth factor and its biological activity. Exp. Mol. Med. 2012; 44(1):1–9. [PubMed: 22228176]

36. Pettersson A, Nagy JA, Brown LF, Sundberg C, Morgan E, Jungles S, Carter R, Krieger JE, Manseau EJ, Harvey VS, et al. Heterogeneity of the Angiogenic Response Induced in Different Normal Adult Tissues by Vascular Permeability Factor/Vascular Endothelial Growth Factor. Lab. Invest. 2000; 80(1):99–115. [PubMed: 10653008]

37. Simons M, Bonow RO, Chronos NA, Cohen DJ, Giordano FJ, Hammond HK, Laham RJ, Li W, Pike M, Sellke FW, et al. Clinical Trials in Coronary Angiogenesis: Issues, Problems, Consensus: An Expert Panel Summary. Circulation. 2000; 102(11):e73–e86. [PubMed: 10982554]

38. Carmeliet P. VEGF gene therapy: stimulating angiogenesis or angioma-genesis? Nat. Med. 2000; 6(10):1102–1103.

39. Lee TT, García JR, Paez JI, Singh A, Phelps EA, Weis S, Shafiq Z, Shekaran A, Del Campo A, García AJ. Light-triggered in vivo activation of adhesive peptides regulates cell adhesion, inflammation and vascularization of biomaterials. Nat. Mater. 2014; 14:352. [PubMed: 25502097]

40. Maess MB, Sendelbach S, Lorkowski S. Selection of reliable reference genes during THP-1 monocyte differentiation into macrophages. BMC Mol. Biol. 2010; 11(1):90. [PubMed: 21122122]

41. Coleman DL, King RN, Andrade JD. The foreign body reaction: a chronic inflammatory response. J. Biomed. Mater. Res. 1974; 8(5):199–211. [PubMed: 4609985]

42. Takahashi H, Wang Y, Grainger DW. Device-based local delivery of siRNA against mammalian target of rapamycin (mTOR) in a murine subcutaneous implant model to inhibit fibrous encapsulation. J. Controlled Release. 2010; 147(3):400–407.

43. Kim J, Dadsetan M, Ameenuddin S, Windebank AJ, Yaszemski MJ, Lu L. In vivo biodegradation and biocompatibility of PEG/sebacic acid-based hydrogels using a cage implant system. J. Biomed. Mater. Res., Part A. 2010; 95(1):191–197.

44. Shao Q, Jiang S. Molecular understanding and design of zwitterionic materials. Adv. Mater. 2015; 27(1):15–26. [PubMed: 25367090]

45. Grainger DW. All charged up about implanted biomaterials. Nat. Biotechnol. 2013; 31(6):507–509. [PubMed: 23752436]

46. Phelps EA, Landázuri N, Thulé PM, Taylor WR, García AJ. Bioartificial matrices for therapeutic vascularization. Proc. Natl. Acad. Sci. U. S. A. 2010; 107(8):3323–3328. [PubMed: 20080569]

47. Phelps EA, García AJ. Engineering more than a cell: vascularization strategies in tissue engineering. Curr. Opin. Biotechnol. 2010; 21(5):704–709. [PubMed: 20638268]

48. Webber MJ, Tongers J, Newcomb CJ, Marquardt K-T, Bauersachs J, Losordo DW, Stupp SI. Supramolecular nanostructures that mimic VEGF as a strategy for ischemic tissue repair. Proc. Natl. Acad. Sci. U. S. A. 2011; 108(33):13438–13443. [PubMed: 21808036]

49. Ehrbar M, Djonov VG, Schnell C, Tschanz SA, Martiny-Baron G, Schenk U, Wood J, Burri PH, Hubbell JA, Zisch AH. Cell-demanded liberation of VEGF121 from fibrin implants induces local and controlled blood vessel growth. Circ. Res. 2004; 94(8):1124–1132. [PubMed: 15044320]

50. Zisch AH, Lutolf MP, Ehrbar M, Raeber GP, Rizzi SC, Davies N, Schmökel H, Bezuidenhout D, Djonov V, Zilla P, et al. Cell-demanded release of VEGF from synthetic, biointeractive cell ingrowth matrices for vascularized tissue growth. FASEB J. 2003; 17(15):2260–2262. [PubMed: 14563693]

51. Meyer J, Whitcomb L, Collins D. Efficient encapsulation of proteins within liposomes for slow release in vivo. Biochem. Biophys. Res. Commun. 1994; 199(2):433–438. [PubMed: 7510952]

52. Scott RC, Rosano JM, Ivanov Z, Wang B, Chong PL-G, Issekutz AC, Crabbe DL, Kiani MF. Targeting VEGF-encapsulated immunoliposomes to MI heart improves vascularity and cardiac function. FASEB J. 2009; 23(10):3361–3367. [PubMed: 19535683]

53. Alemdaro lu C, Degim Z, Celebi N, Sengezer M, Alömeroglu M, Nacar A. Investigation of epidermal growth factor containing liposome formulation effects on burn wound healing. J. Biomed. Mater. Res., Part A. 2008; 85(1):271–283.

54. Segers VFM, Lee RT. Local delivery of proteins and the use of self-assembling peptides. Drug Discovery Today. 2007; 12(13–14):561–568. [PubMed: 17631251]

55. Miller RE, Kopesky PW, Grodzinsky AJ. Growth factor delivery through self-assembling peptide scaffolds. Clin. Orthop. Relat. Res. 2011; 469(10):2716–2724. [PubMed: 21503788]

56. Schneider A, Garlick JA, Egles C. Self-assembling peptide nanofiber scaffolds accelerate wound healing. PLoS One. 2008; 3(1):e1410. [PubMed: 18183291]

57. Hsieh PCH, Davis ME, Gannon J, MacGillivray C, Lee RT. Controlled delivery of PDGF-BB for myocardial protection using injectable self-assembling peptide nanofibers. J. Clin. Invest. 2006; 116(1):237–248. [PubMed: 16357943]

58. Segers VFM, Tokunou T, Higgins LJ, MacGillivray C, Gannon J, Lee RT. Local delivery of protease-resistant stromal cell derived factor-1 for stem cell recruitment after myocardial infarction. Circulation. 2007; 116(15):1683–1692. [PubMed: 17875967]

59. Davis ME, Hsieh PCH, Takahashi T, Song Q, Zhang S, Kamm RD, Grodzinsky AJ, Anversa P, Lee RT. Local myocardial insulin-like growth factor 1 (IGF-1) delivery with biotinylated peptide nanofibers improves cell therapy for myocardial infarction. Proc. Natl. Acad. Sci. U. S. A. 2006; 103(21):8155–8160. [PubMed: 16698918]

60. Franssen O, Vandervennet L, Roders P, Hennink WE. Degradable dextran hydrogels: controlled release of a model protein from cylinders and microspheres. J. Controlled Release. 1999; 60(2–3): 211–221.

61. Nasongkla N, Bey E, Ren J, Ai H, Khemtong C, Guthi JS, Chin S-F, Sherry AD, Boothman DA, Gao J. Multifunctional polymeric micelles as cancer-targeted, MRI-ultrasensitive drug delivery systems. Nano Lett. 2006; 6(11):2427–2430. [PubMed: 17090068]

62. Lee JS, Go DH, Bae JW, Lee SJ, Park KD. Heparin conjugated polymeric micelle for long-term delivery of basic fibroblast growth factor. J. Controlled Release. 2007; 117(2):204–209.

63. Chappell JC, Song J, Burke CW, Klibanov AL, Price RJ. Targeted delivery of nanoparticles bearing fibroblast growth factor-2 by ultrasonic microbubble destruction for therapeutic arteriogenesis. Small. 2008; 4(10):1769–1777. [PubMed: 18720443]

64. Zhang S, Uluda H. Nanoparticulate systems for growth factor delivery. Pharm. Res. 2009; 26(7): 1561–1580. [PubMed: 19415467]

65. Zisch AH, Schenk U, Schense JC, Sakiyama-Elbert SE, Hubbell JA. Covalently conjugated VEGF −fibrin matrices for endothelialization. J. Controlled Release. 2001; 72(1–3):101–113.

66. Chen F-M, Zhang M, Wu Z-F. Toward delivery of multiple growth factors in tissue engineering. Biomaterials. 2010; 31(24):6279–6308. [PubMed: 20493521]

67. Fujita M, Ishihara M, Simizu M, Obara K, Ishizuka T, Saito Y, Yura H, Morimoto Y, Takase B, Matsui T, et al. Vascularization in vivo caused by the controlled release of fibroblast growth factor-2 from an injectable chitosan/non-anticoagulant heparin hydrogel. Biomaterials. 2004; 25(4):699–706. [PubMed: 14607508]
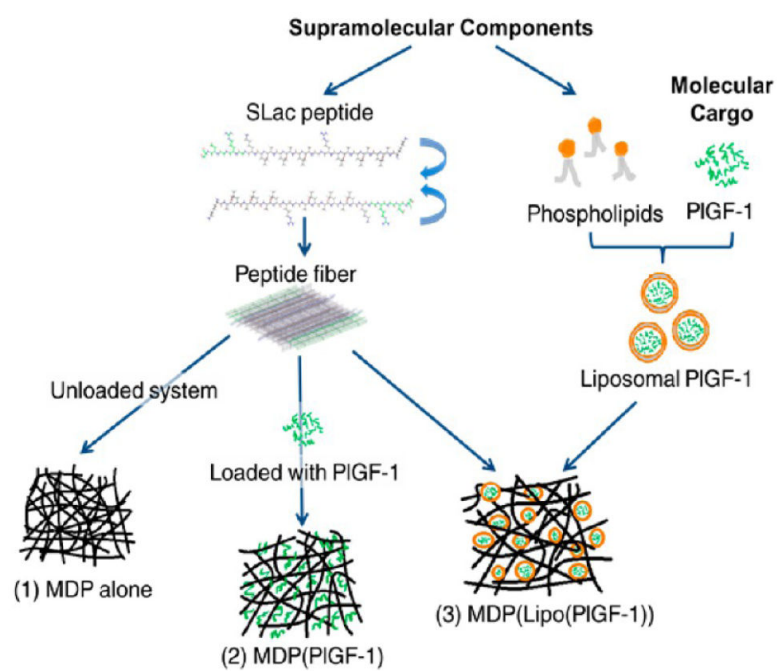
Figure 1.
Supramolecular orthogonal self-assembly. Schematic showing individual components that self-assemble to yield three different hydrogels (1–3).
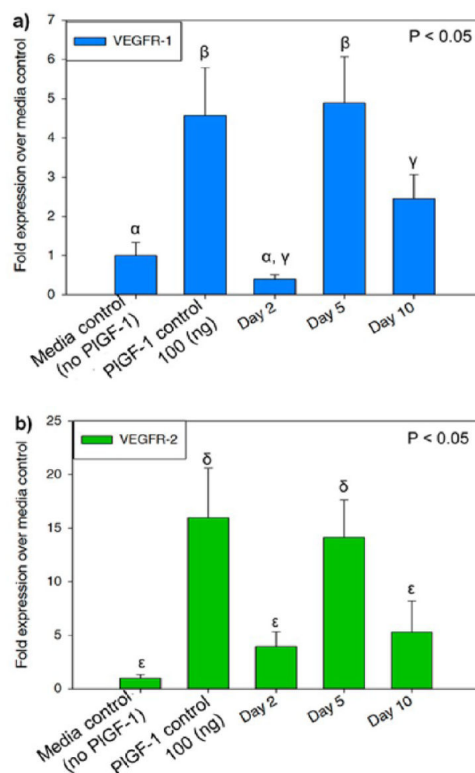
Figure 2.
Angiogenic receptor activation as a function of temporal growth factor release. Quantitative RT-PCR showing expression levels of (a) VEGFR-1 and (b) VEGFR-2 in HUVECs at day 2, day 5, and day 10 time points; fold expression over media control. HUVECs were treated with release aliquots from MLCs containing PlGF-1 encapsulated liposomes to induce expression of angiogenic markers. MLCs refer to Multidomain peptide–Liposome Composites. Different Greek letters indicate statistically significant differences between each receptor.
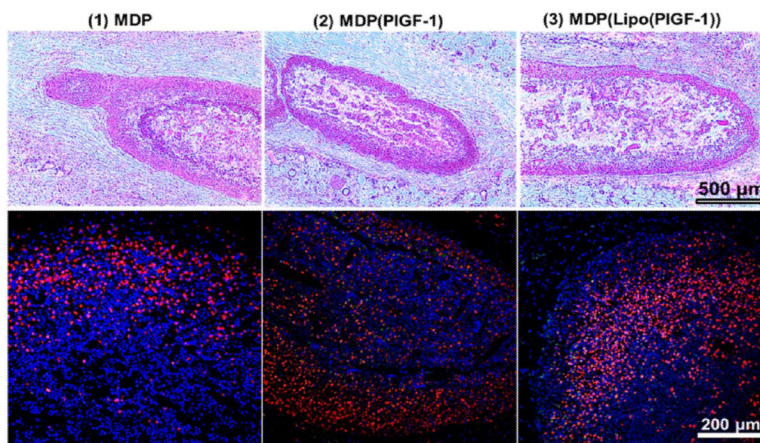
Figure 3.
Evaluation of cellular infiltrate. Top row: H&E images of subcutaneous implants in rats at day 2, showing rapid cellular infiltration (days 5 and 10 H&E images are shown in Figure S3); scale bar 500 μm. Bottom row: Immunostaining for monocytes/macrophages (CD68+; red) and nuclei (DAPI; blue) within the various implants at day 2. High macrophage infiltration can be seen in all cases (days 5 and 10 images are shown in Figures S4); scale bar 200 μm.
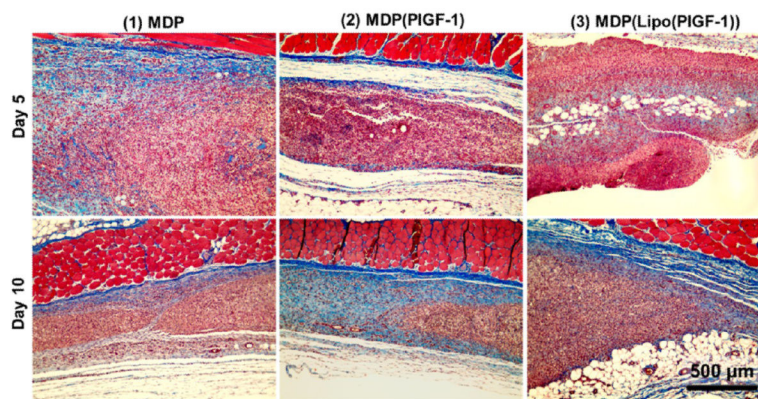
Figure 4.
Evaluation of new matrix formation. Masson's Trichrome staining of subcutaneous implants in rats showing deposition of new collagen matrix at day 5 (top row). By day 10 (bottom row), significant degradation of peptide matrix is observed, with new collagen matrix deposited where the implant material existed previously. Masson's Trichrome stain indicates muscle fibers in red, collagen in blue, cell cytoplasm in pink, and cell nuclei in dark brown. Scale bar 500 μm.
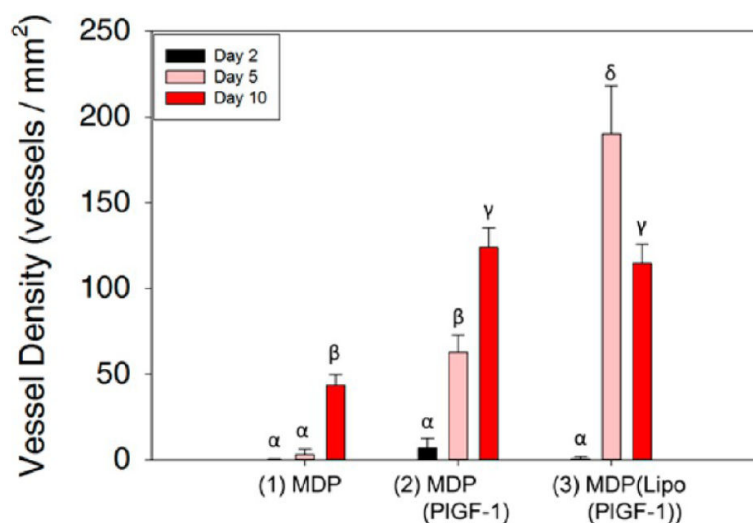
Figure 5.
Quantification of angiogenesis. Vessel density in the three implants was analyzed showing
the significant effect of liposomal PlGF-1 release from MLCs on angiogenesis. At day 2, no
vessel development is observed, while at day 5, the highest vessel density is seen in (3). At
day 10, vessel density stabilizes in (3) due to loss of immature vessels, while it finally starts
to increase in (1). A moderate increase in vessel density is seen in (2) from day 5 to day 10.
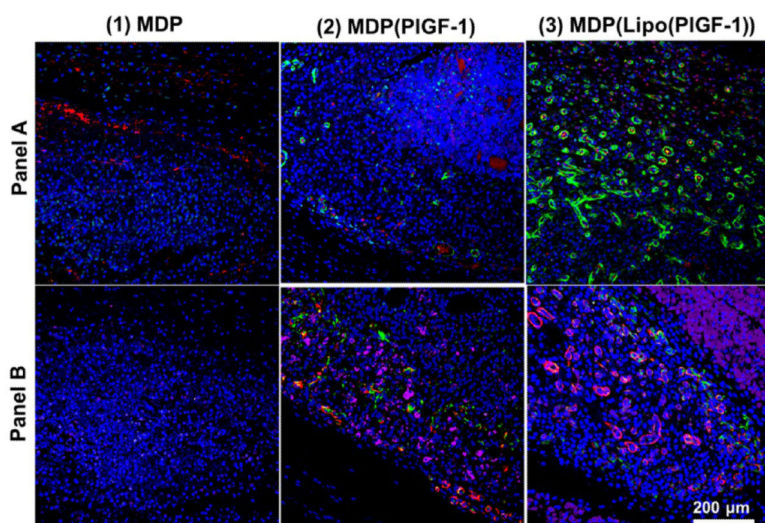Different Greek letters indicate statistically significant differences.

Figure 6.
Assessment of neoangiogenesis: day 5 time point. Two panels of angiogenic markers were used for qualifying vessel development: (A) endothelial marker (vWF+; red), smooth muscle marker (a-SMA+; green) counterstained with DAPI; (B) endothelial marker (Lectin +; purple), pericyte marker (Nestin+; green), smooth muscle marker (a-SMA+; red) counterstained with DAPI. Both panels show development of mature vasculature by day 5 in the presence of PlGF-1. Scale bar 200 μm.
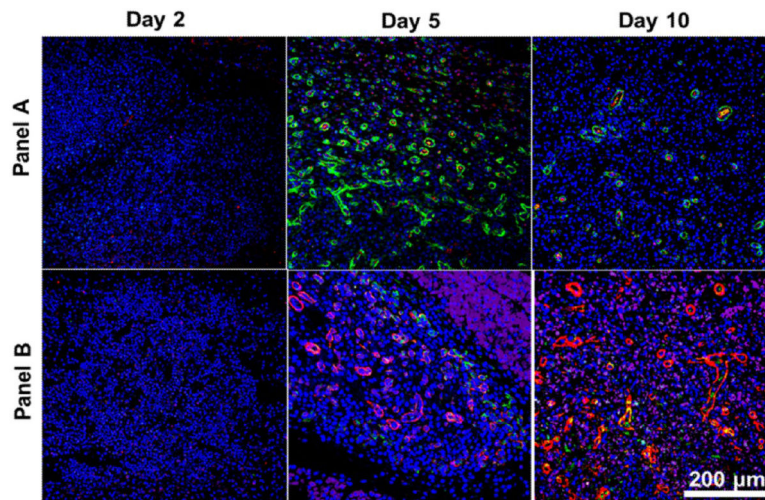
Figure 7.
Assessment of neoangiogenesis: MDP(Lipo(PlGF-1)). The degree of liposomal PlGF-1-dependent vessel development at each time point can be seen in these images. At day 5, vigorous vessel formation is observed. By day 10, mature vessels remain intact while the immature ones resorb, giving a stabilized vascular network. Two panels of angiogenic markers were used for qualifying vessel development: (A) endothelial marker (vWF+; red), smooth muscle marker (a-SMA+; green) counterstained with DAPI; (B) endothelial marker (Lectin+; purple), pericyte marker (Nestin+; green), smooth muscle marker (a-SMA+; red) counterstained with DAPI. Scale bar 200 μm (component images are shown in Figure S6, and images for all other implants are shown in Figures S7 and S8).
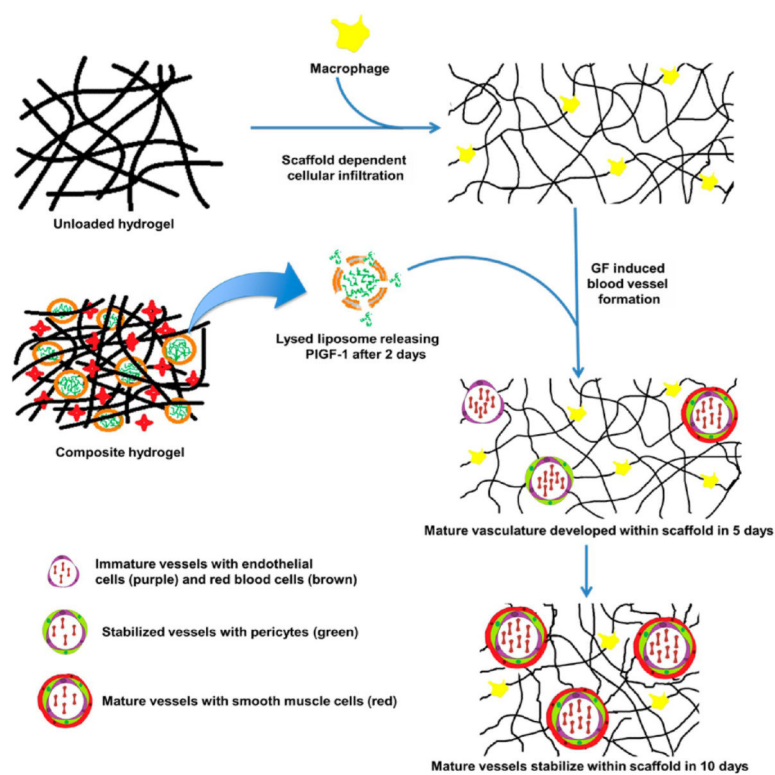
Figure 8.
Schematic of proposed in vivo mechanism. Orthogonally self-assembled scaffolds recruit macrophages and release growth factors. Macrophages recruited to the implant resolve over the implant period, seguing the development of endothelial lined vessels (day 2) with supporting pericytes (day 5) and maturation into smooth-muscle-lined vessels (days 5–10).

Table 1

Summary of Composite Hydrogels and MDP-Liposome Composites (MLCs)[a]

	day 2		day 5		day 10	
	nascent vessels	mature vessels	nascent vessels	mature vessels	nascent vessels	mature vessels
MDP	0	0	0	0	2	1
MDP(PlGF-1)	1	0	2	0	2	2
MDP(Lipo (PlGF-1))	0	0	2	3	1	3

[a]Numbers indicate degree of response: 1 = low vessel density, 2 = moderate vessel density, 3 = high vessel density.